



Cancer Research

Trastuzumab Reverses Letrozole Resistance and Amplifies the Sensitivity of Breast Cancer Cells to Estrogen

Gauri Sabnis, Adam Schayowitz, Olga Goloubeva, et al.

Cancer Res 2009;69:1416-1428. Published OnlineFirst February 3, 2009.

Updated version Access the most recent version of this article at:
doi:[10.1158/0008-5472.CAN-08-0857](https://doi.org/10.1158/0008-5472.CAN-08-0857)

Cited Articles This article cites by 41 articles, 21 of which you can access for free at:
<http://cancerres.aacrjournals.org/content/69/4/1416.full.html#ref-list-1>

Citing articles This article has been cited by 15 HighWire-hosted articles. Access the articles at:
<http://cancerres.aacrjournals.org/content/69/4/1416.full.html#related-urls>

E-mail alerts [Sign up to receive free email-alerts](#) related to this article or journal.

Reprints and Subscriptions To order reprints of this article or to subscribe to the journal, contact the AACR Publications Department at pubs@aacr.org.

Permissions To request permission to re-use all or part of this article, contact the AACR Publications Department at permissions@aacr.org.

Trastuzumab Reverses Letrozole Resistance and Amplifies the Sensitivity of Breast Cancer Cells to Estrogen

Gauri Sabnis,¹ Adam Schayowitz,¹ Olga Goloubeva,² Luciana Macedo,¹ and Angela Brodie^{1,2}

¹Department of Pharmacology and Experimental Therapeutics, University of Maryland Baltimore; ²University of Maryland Greenebaum Cancer Center, Baltimore, Maryland

Abstract

In this study, we investigated adaptive mechanisms associated with aromatase inhibitor (AI) resistance in breast cancer cells and show that sensitivity to AIs can be extended through dual inhibition of estrogen receptor (ER) and human epidermal receptor-2 (Her-2) signaling. We used human ER-positive breast cancer cells stably transfected with the aromatase gene (MCF-7Ca). These cells grow as tumors in nude mice and are inhibited by AIs. Despite continued treatment, tumors eventually become insensitive to AI letrozole. The cells isolated from these long-term letrozole-treated tumors (LTLT-Ca) were found to have decreased ER α levels. Our results suggest that LTLT-Ca cells survive estrogen deprivation by activation of Her-2/mitogen-activated protein kinase (MAPK) pathway. Here, we show that trastuzumab (antibody against Her-2; IC₅₀ = 0.4 mg/mL) was very effective in restoring the ER α levels and sensitivity of LTLT-Ca cells to endocrine therapy by down-regulation of Her-2/MAPK pathway and up-regulation of ER α . In contrast, trastuzumab was ineffective in the parental hormone-responsive MCF-7Ca cells (IC₅₀ = 4.28 mg/mL) and xenografts. By blocking Her-2, trastuzumab also up-regulates ER α and aromatase expression and hypersensitized MCF-7Ca cells to E₂. We show that trastuzumab is beneficial in hormone-refractory cells and xenografts by restoring ER, implicating Her-2 as a negative regulator of ER α . In xenograft studies, the combination of trastuzumab plus letrozole is equally effective in inhibiting growth of MCF-7Ca tumors as letrozole alone. However, on the acquisition of resistance and increased Her-2 expression, the combination of letrozole plus trastuzumab provided superior benefit over letrozole or trastuzumab alone. [Cancer Res 2009;69(4):1416–28]

Introduction

Aromatase inhibitors (AI) such as letrozole and anastrozole that reduce estrogen production have now been shown to be more effective than antiestrogen (AE) tamoxifen in estrogen receptor-positive (ER⁺) breast cancer patients and have few side effects. Nevertheless, not all patients respond and resistance to treatment

may eventually occur in others. To investigate the mechanisms involved in the loss of sensitivity of the tumors to AIs, we developed a cell line isolated from tumors of human ER⁺ breast cancer cells (MCF-7) stably transfected with aromatase (MCF-7Ca) grown in mice treated with letrozole for an extended period of time (1–3). We have previously reported that during treatment with letrozole, MCF-7Ca xenografts up-regulate human epidermal receptor-2 (Her-2) and proteins in the downstream mitogen-activated protein kinase (MAPK) signaling pathway (1). These cells also exhibited lower expression of ER α and apparent “estradiol-independent” growth. We have also shown that signaling pathways, such as the Her-2/MAPK, are key regulators of the growth of letrozole-refractory cells (1, 4). Similarly, several other investigators have reported the importance of members of epidermal growth factor receptor (EGFR) family (Her-2/EGFR) in resistance to endocrine therapy (5–8). We and others have suggested that the combination of EGFR/Her-2 tyrosine kinase inhibitors or trastuzumab (monoclonal humanized antibody against Her-2, Herceptin) in combination with AIs or AEs may delay acquisition of resistance (4, 9–13).

In this study, we investigated the effects of trastuzumab on the growth of letrozole-refractory breast cancer cells. On examination, MCF-7Ca–derived tumors treated with letrozole up-regulated Her-2 4 weeks into treatment despite continued responsiveness to letrozole. Moreover, the level of Her-2 protein was found to be 6-fold higher in letrozole-refractory tumors than the control tumors (1). However, when Her-2 was inhibited, ER α levels were restored. This suggests that Her-2 is a negative regulator of ER α . This observation led to our hypothesis that inhibition of both the Her-2 and estrogen signaling pathways is required to prolong the responsiveness of the tumors to endocrine therapies (14, 15).

Thus, the combination of an AI plus Her-2 inhibitor could provide a substantial benefit in tumor growth inhibition when used after the acquisition of letrozole resistance.

Materials and Methods

Materials. DMEM, modified improved MEM (IMEM), penicillin/streptomycin solution (10,000 IU each), 0.25% trypsin–1 mmol/L EDTA solution, Dulbecco's PBS (DPBS), and geneticin (G₄₁₈) were obtained from Invitrogen. Androstenedione (Δ^4 A), tamoxifen, and Matrigel were obtained from Sigma Chemical Co. Antibodies against Her-2 and phosphorylated Her-2 (p-Her-2) were purchased from Upstate (now Millipore) and antibodies against phosphorylated MAPK (p-MAPK), MAPK, phosphorylated Elk-1 (p-Elk-1), and phosphorylated p90RSK (p-p90RSK) were purchased from Cell Signaling Technology. Antibodies against ER α , and aromatase (CYP-19) were purchased from Santa Cruz Biotechnology. Radioactive ligands for ER-binding assay and aromatase assay, ³H-E₂ (40 Ci/mmol), and ³H- Δ^4 A (23.5 Ci/mmol) were purchased from Perkin-Elmer.

MCF-7 human breast cancer cells stably transfected with the human aromatase gene (MCF-7Ca) were provided by Dr. S. Chen (City of Hope,

Note: Novartis Pharma (Basel, Switzerland) supplied the letrozole used in this study. This work was also presented in part at the Centennial AACR Meeting, Los Angeles, CA, April 2007; 29th San Antonio Breast Cancer Symposium, San Antonio, TX, December 2006; and XIIIth International Aromatase Meeting, Baltimore, MD, September 2006.

Requests for reprints: Angela Brodie, Department of Pharmacology and Experimental Therapeutics, University of Maryland, School of Medicine, Health Science Facility I, Room 580G, 685 West Baltimore Street, Baltimore, MD 21201. Phone: 410-706-3137; Fax: 410-706-0032; E-mail: abrodie@umaryland.edu.

©2009 American Association for Cancer Research.
doi:10.1158/0008-5472.CAN-08-0857

Duarte, CA). Letrozole was provided by Dr. D. Evans (Novartis Pharma, Basel, Switzerland). The pure AE fulvestrant and anastrozole were supplied by Dr. E. Anderson (AstraZeneca Pharmaceuticals, Macclesfield, United Kingdom).

Cell culture. MCF-7Ca cells were routinely cultured in DMEM supplemented with 5% fetal bovine serum, 1% penicillin/streptomycin, and 700 $\mu\text{g}/\text{mL}$ G₄₁₈. LTLT-Ca cells were developed from MCF-7Ca cells as described earlier from tumors of mice treated with letrozole for 56 wk (1). The cells were maintained in steroid-depleted medium, which consisted of phenol red-free IMEM supplemented with 5% dextran-coated charcoal-treated serum, 1% penicillin/streptomycin, and 750 $\mu\text{g}/\text{mL}$ G₄₁₈ and 1 $\mu\text{mol}/\text{L}$ letrozole. Cell proliferation assays were performed using the 3-(4,5-dimethylthiazol-2-yl)-2,5-diphenyltetrazolium bromide (MTT) assay as described earlier (4). The results were expressed as a percentage of the cell number in the $\Delta^4\text{A}$ -treated control wells. IC₅₀ values for inhibitors were calculated from the linear regression line of the plot of percentage inhibition versus log inhibitor concentration.

Tumor growth in ovariectomized female athymic nude mice. All animal studies were performed according to the guidelines and approval of the Animal Care Committee of the University of Maryland, Baltimore. Female ovariectomized BALB/c athymic nude mice 4 to 6 wk of age were obtained from the National Cancer Institute-Frederick Cancer Research and Development Center (Frederick, MD). The mice were housed in a pathogen-free environment under controlled conditions of light and humidity and received food and water *ad libitum*.

The tumor xenografts of MCF-7Ca cells were grown in the mice as previously described (1, 16, 17). Each mouse received s.c. inoculations in one site per flank with 100 μL of cell suspension containing $\sim 2.5 \times 10^7$ cells. The mice were injected daily with $\Delta^4\text{A}$ (100 $\mu\text{g}/\text{d}$). Weekly tumor measurements and treatments began when the tumors reached $\sim 300 \text{ mm}^3$. Mice were assigned to groups for treatment so that there was no statistically significant difference in tumor volume among the groups at the beginning of treatment. Letrozole and $\Delta^4\text{A}$ for injection were prepared in 0.3% hydroxypropylcellulose. Trastuzumab for injection was prepared as 20 mg/mL stock solution in bacteriostatic water for injection and then diluted in 0.9% NaCl solution to obtain the required concentrations. Mice were then injected s.c. five times weekly with the indicated drugs: 100 $\mu\text{g}/\text{mouse}/\text{d}$ $\Delta^4\text{A}$ plus 10 $\mu\text{g}/\text{mouse}/\text{d}$ letrozole or 10 $\mu\text{g}/\text{mouse}/\text{d}$ letrozole plus trastuzumab or 100 $\mu\text{g}/\text{mouse}/\text{d}$ $\Delta^4\text{A}$ plus trastuzumab for indicated time. The doses of letrozole and $\Delta^4\text{A}$ used are as previously determined and reported (1, 2). Mice in the trastuzumab group received 5 mg/kg/wk of the drug i.p. divided in two doses. Mice in the $\Delta^4\text{A}$ and trastuzumab group were treated for 7 wk, after which they were sacrificed due to large tumor volumes by decapitation and the blood was collected for analysis. The other groups (letrozole, trastuzumab plus letrozole, letrozole switched to trastuzumab plus letrozole, and letrozole switched to trastuzumab) were sacrificed on week 28.

Western blotting. The protein extracts from tumor tissues were prepared by homogenizing the tissue in ice-cold DPBS containing protease inhibitors (18). A total of 50 μg protein from each sample was analyzed by SDS-PAGE as described previously (4). Bands were quantitated by densitometry using Molecular Dynamics Software (ImageQuant). The densitometric values are corrected for loading control.

Competitive binding studies. Binding of trastuzumab to ER in MCF-7Ca cells was assessed by competitive binding assay as described before (3). MCF-7Ca cells were transferred to steroid-depleted medium for 1 d before plating for the binding assay. $^3\text{H-E}_2$ was used as a ligand and non-radiolabeled E_2 was used to determine nonspecific binding. Triamcinolone (1 $\mu\text{mol}/\text{L}$) was used to saturate glucocorticoid receptors.

$^3\text{H}_2\text{O}$ release assay for aromatase activity measurement. The radiometric $^3\text{H}_2\text{O}$ release assay was performed as described previously (19). For pretreatment studies, cells were treated with indicated agent for 24 h before incubating with [$1\text{-}\beta\text{-}^3\text{H}$] $\Delta^4\text{A}$ for 18 h. For measuring aromatase activity in tumor samples, the tumors were homogenized in ice-cold DPBS. The resulting homogenate was used for aromatase activity assay (19). The activity of the enzyme is corrected for protein concentration in the tumor homogenates and cells.

ER α transactivation assay. To measure activation of ER α , an ELISA-based ER transactivation assay was performed as per manufacturer's guidelines (Panomics). Briefly, the nuclear lysates of cells or tumors were generated as described by the manufacturer. Activated ER from nuclear extracts was allowed to bind to an ER consensus binding site (ER probe) on a biotinylated oligonucleotide. These oligonucleotides were then immobilized on a streptavidin-coated 96-well plate. The ER bound to the oligonucleotide is then detected by an antibody directed against ER. An additional horseradish peroxidase-conjugated secondary antibody provided colorimetric readout quantified by reading absorbance at 450 nm.

RNA extraction and reverse transcription. RNA was extracted and purified using the RNeasy Mini kit (Qiagen) as per manufacturer's protocol. Total RNA concentration and purity were determined from 260 and 280 nm absorbances. RNA was diluted with water to 0.08 $\mu\text{g}/\mu\text{L}$ and reverse transcribed as described by Kazi and colleagues (20).

PCR. Analysis of ER α , CYP-19, and pS2 mRNA expression was done by conventional PCR. Each 30 μL reaction consisted of 3 μL reverse transcriptase, 3 μL $10\times$ buffer, 2.4 μL deoxynucleotide triphosphate mix, 3 μL 5 $\mu\text{mol}/\text{L}$ primer mix, 0.15 μL Taq DNA polymerase (Qiagen), and 18.45 μL molecular biology-grade water. The following primers were used for the PCR analysis: *human pS2*, 5'-ACCATGGAGAACAAGGTGAT-3' (forward) and 5'-AAATTCACACTCCTCTTCTG-3' (reverse; ref. 21); *human ER α* , 5'-GATCCTTCTAGACCCTTCAGTG-3' (forward) and 5'-TCTTCCAGAGACTTCAAGGTGCT (reverse); *human CYP-19*, 5'-GAATATTGGAAGATGCACAGACT-3' (forward) and 5'-GGGTAAGATCATTTCCAGCATGT-3' (reverse; refs. 19, 22); and *human 18s rRNA*, 5'-CAACTTTCGATGGTAGTCGC-3' (forward) and 5'-CGCTATTGGAGCTGGAATTAC-3' (reverse; ref. 20).

ChIP assay. For *in vitro* ChIP assay, the treated cells were washed with DPBS and fixed with 1% formaldehyde/DPBS for 10 min at 37°C, after which the cells were washed with ice-cold DPBS containing protease inhibitors. The cells were collected into 1 mL DPBS and pelleted by centrifugation at 6,000 rpm for 5 min at 4°C. The cell pellet was resuspended in nuclear lysis buffer (ChIP kit, Upstate) and incubated on ice for 15 min.

For *in vivo* ChIP assay, tumor slices were immersed in 2% formaldehyde/DPBS mixture and incubated at room temperature for 15 min. Fixation was stopped by adding 1 mol/L glycine and incubating for 5 min at room temperature. The tissues were rinsed in ice-cold DPBS containing the protease inhibitor tablet and homogenized on ice in modified radio-immunoprecipitation assay buffer. The tissue homogenate was centrifuged at 12,000 rpm for 5 min at 4°C; the nuclear pellet was resuspended in nuclear lysis buffer and incubated on ice for 15 min. Samples were sonicated on ice for 10×10 s cycles, with 20-s pauses between each cycle. The sonicated samples were centrifuged at 14,000 rpm for 10 min at 4°C. Sonicated samples were diluted 1:10 with dilution buffer (ChIP kit) before being immunocleared in a solution containing protein A- or G-Sepharose slurry (Amersham) in Tris/EDTA buffer, salmon sperm DNA (Invitrogen), and normal mouse or rabbit serum (Sigma Chemical) for 2 h at 4°C. Immunocleared supernatants were incubated overnight at 4°C with anti-ER α antibody (Santa Cruz Biotechnology). Protein A- or G-Sepharose beads and salmon sperm DNA were then added and incubated for 1 h at 4°C. The beads were then washed sequentially with 1 mL each of wash buffers. The protein-DNA complexes were then eluted by twice incubating beads in elution buffer for 10 min at room temperature with vigorous mixing. To separate immunoprecipitated protein and DNA, the pooled elutes were incubated at 65°C overnight. The DNA was purified using the QIAquick PCR Purification kit (Qiagen). Alternatively, immunoprecipitated ER α on the beads was subjected to Western immunoblotting. The boiled (denatured) protein samples were resolved by SDS-PAGE and membranes were probed for histone H3 and RNA polymerase II.

The yield of target region DNA in each sample after ChIP was analyzed by conventional PCR. The following primers were used for PCR analysis (34 cycles at 60°C annealing temperature): *human pS2*, 5'-GGCCATCTCTCACTATGAATC-3' (forward) and 5'-GGCAGGCTCTGTTTGTCTTAAA-3' (reverse; ref. 20); *human CYP-19 Promoter 1.3/II*, 5'-CGGAGTCAACGATTTGGTCGTAT-3' (forward) and 5'-AGCCTTCTCCATGGTGGTGAA-GAC-3' (reverse; ref. 23).

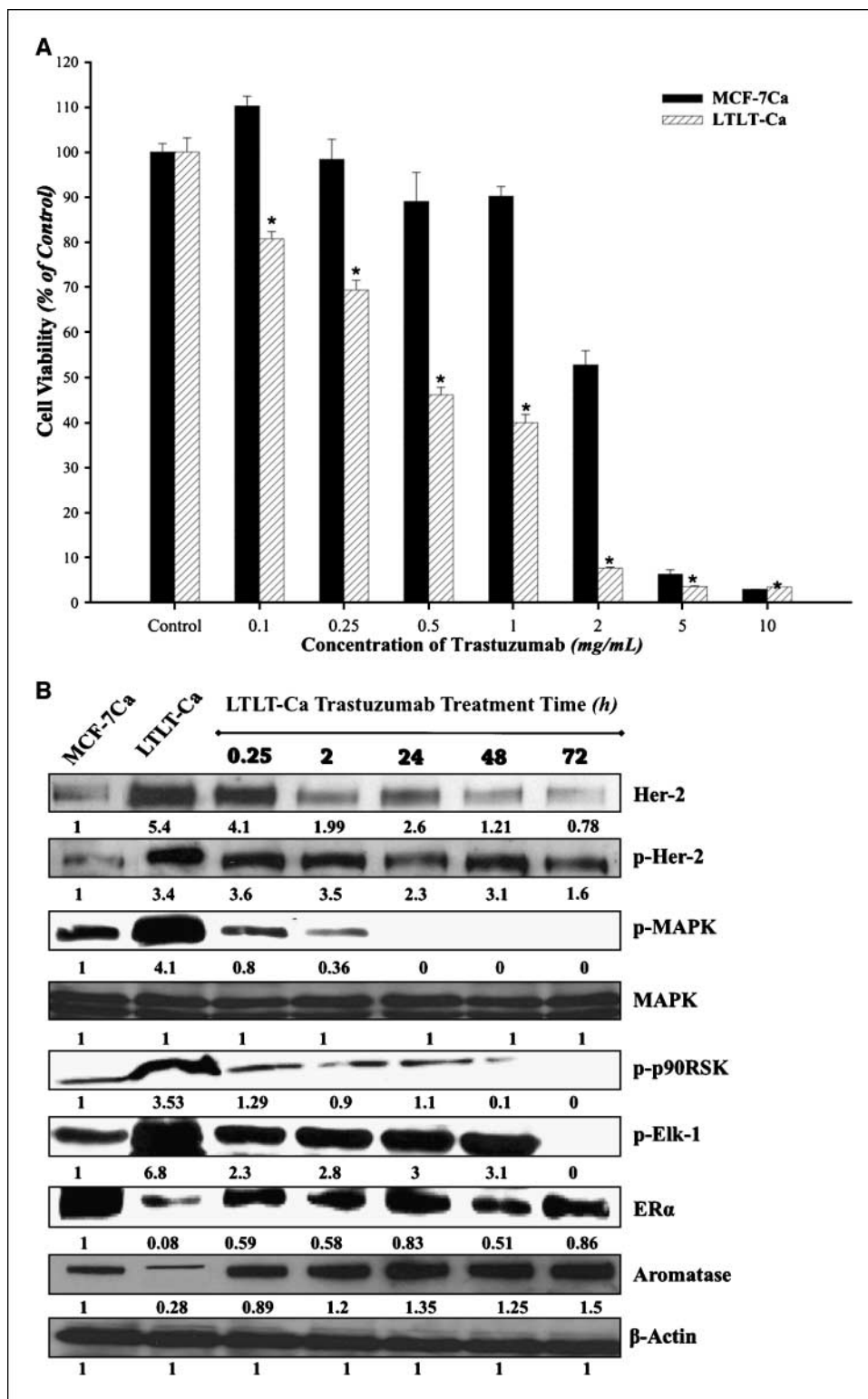


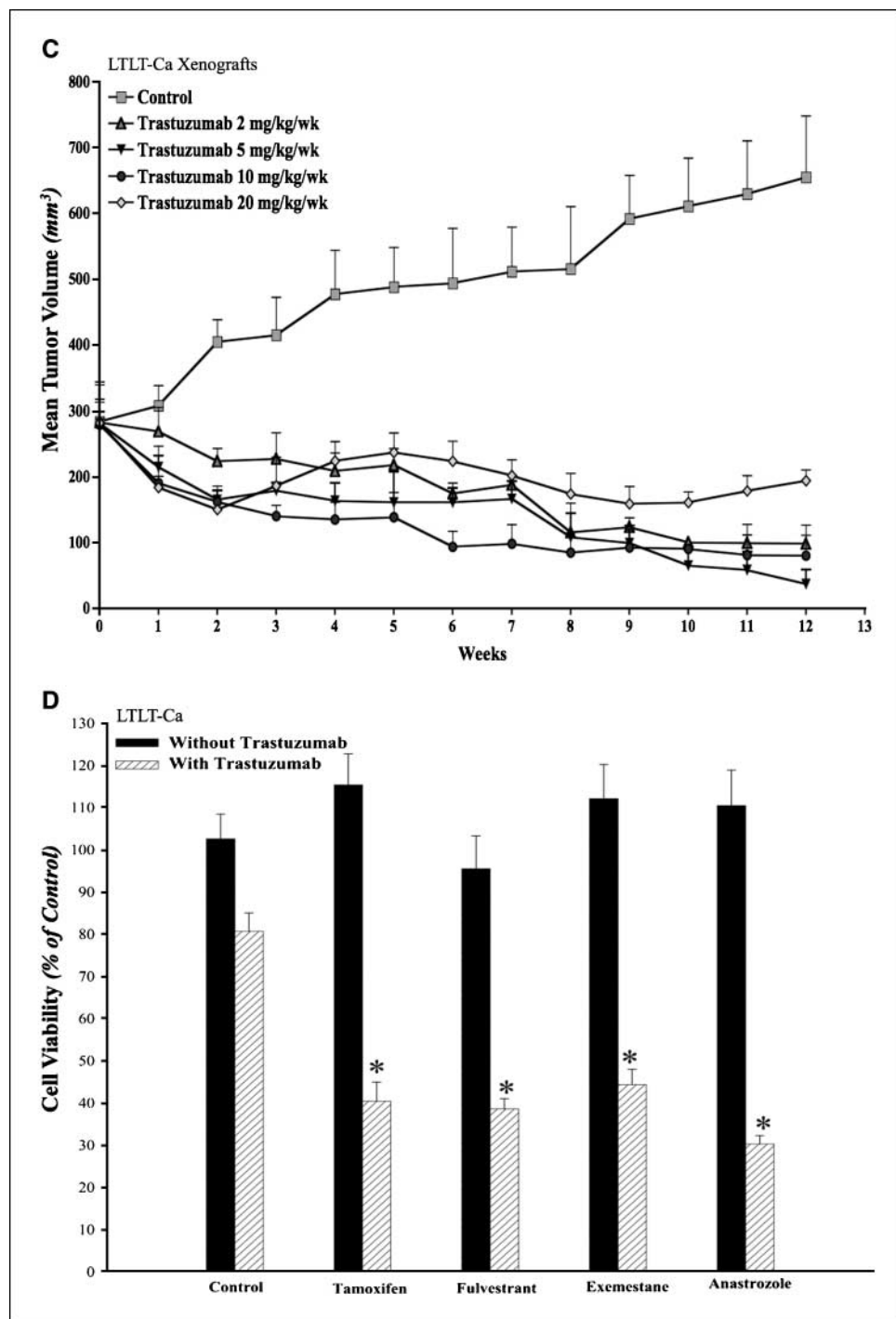
Figure 1. A, effect of trastuzumab on proliferation of MCF-7Ca and LTLT-Ca cells *in vitro*. Viability of cells was measured by MTT assay after 6-d treatment with trastuzumab as described in Materials and Methods. The treatment with trastuzumab is significantly more effective in reducing cell viability of LTLT-Ca cells compared with MCF-7Ca cells at all doses. At each dose of trastuzumab tested (0.1–10 mg/mL) in LTLT-Ca cells, growth was inhibited significantly better (*, $P < 0.0001$) than in MCF-7Ca cells. B, effect of trastuzumab treatment at various time points on the expression of protein in the Her-2/MAPK pathway, ER α , and aromatase in LTLT-Ca cells. Expression of proteins was examined using Western immunoblotting as described in Materials and Methods. Blot shows Her-2, p-Her-2 at 185 kDa, p-MAPK, MAPK at 42 to 44 kDa, p-p90RSK at 90 kDa, p-Elk-1 at 41 kDa, ER α at 66 kDa, aromatase at 55 kDa, and β -actin at 45 kDa. The blots show a single representative of three independent experiments.

The promoter that was analyzed was I.3/II, which is the main aromatase promoter used in breast cancer cell lines such as MCF-7 (24) and thus measures the effect of trastuzumab on endogenous aromatase in MCF-7 cells. The MCF-7Ca cells contain human placental aromatase cDNA (placental CYP-19 uses promoter I.1 and I.2; ref. 25).

Statistics. For *in vivo* studies, mixed-effects models were used. The tumor volumes were analyzed with S-PLUS (7.0; Insightful Corp.) to

estimate and compare an exponential variable (β_i) controlling the growth rate for each treatment groups. The original values for tumor volumes were log transformed. In the process of searching for a suitable model, we observed that the piecewise (knot at 15 wk) model fits the data reasonably well (on groups switched after week 15 to another drug). The spline model with a single knot at time = week-15 wk was used to accommodate the nonlinearity with a piece-wise linear model.

Figure 1. Continued. C, effect of trastuzumab treatment at various doses on the growth of LTLT-Ca xenografts. LTLT-Ca xenografts were grown in female OVX nude mice as described in Materials and Methods. The mice in the control and letrozole-treated group exhibited similar rate of tumor growth. The difference in the exponential variable governing growth was -0.027 ($P = 0.71$) over first 8 wk and 0.001 ($P = 0.97$) over 19 wk. Four doses of trastuzumab were tested. All of the tested doses caused a marked regression of LTLT-Ca xenografts. The growth rate of tumors of mice treated with trastuzumab (5 mg/kg/wk) was significantly different from mice in the control ($P = 0.0008$) and letrozole-treated ($P = 0.0002$) mice. The difference in the exponential variable governing growth between control and trastuzumab was 0.24 ($P = 0.0008$). The difference in the exponential variable governing growth between letrozole and trastuzumab was 0.27 ($P = 0.0002$). **D,** effect of combination of trastuzumab with AEs tamoxifen and fulvestrant and AIs exemestane and anastrozole in LTLT-Ca cells. Viability of cells was measured by MTT assay after 6-d treatment with AEs and AIs in the presence or absence of $100 \mu\text{g/mL}$ trastuzumab as described in Materials and Methods. The generalized linear model method was applied to estimate and assess differences among groups' means. The cell viability was found to be significantly lower in treatment groups treated with the combination of trastuzumab plus AI or AE versus control (*, $P < 0.0001$) or trastuzumab alone (*, $P < 0.0001$) or the endocrine agent alone (*, $P < 0.0001$).



All P values < 0.05 were considered statistically significant. The graphs are represented as mean \pm SE.

Results

Trastuzumab inhibits growth of LTLT-Ca cells and tumors and down-regulates MAPK activation. Trastuzumab was found to inhibit growth of LTLT-Ca cells in a dose-dependent manner with an IC_{50} of $400 \mu\text{g/mL}$ ($2.75 \mu\text{mol/L}$) compared with 4.28 mg/mL ($29.41 \mu\text{mol/L}$) in parental MCF-7Ca cells (Fig. 1A).

In LTLT-Ca cells, trastuzumab ($100 \mu\text{g/mL}$) also decreased the activation of proteins of the MAPK pathway along with Her-2 in a time-dependent manner (Fig. 1B). This down-regulation was initiated as early as 15 minutes and was sustained until at least 72 hours. In addition, $\text{ER}\alpha$ was nearly restored to the level of the parental MCF-7Ca cells.

To study the effect of trastuzumab *in vivo*, LTLT-Ca cells were inoculated s.c. into ovariectomized nude mice. The following day, the mice were divided in two groups. One group received letrozole ($n = 5$) and the other group received vehicle only (control, $n = 25$).

When the tumors of the mice in the control group reached $\sim 300 \text{ mm}^3$, this group was regrouped into five ($n = 5$) and injected with vehicle or 2, 5, 10, and 20 mg/kg/wk of trastuzumab i.p. (divided in two doses). As shown in Fig. 1C, the tumors in all of the trastuzumab-treated groups regressed over the course of the experiment. The dose of 5 mg/kg/wk trastuzumab was selected for future investigations. As shown previously (1), treatment with letrozole did not result in a statistically significant difference in tumor growth than observed in controls ($P = 0.91$).

Trastuzumab restores sensitivity of LTLT-Ca cells to AEs and AIs. As shown in our earlier studies, LTLT-Ca cells exhibit cross-resistance to growth-inhibitory effects of tamoxifen, fulvestrant, exemestane, and anastrozole (1). However, the combination of trastuzumab (100 $\mu\text{g}/\text{mL}$) with AEs or AIs produced synergistic growth inhibition. As shown in Fig. 1D, the combination of trastuzumab with AE/AI at 1 $\mu\text{mol}/\text{L}$ each produced synergistic

growth inhibition. The combination was statistically better than either drug alone ($P < 0.0001$) or control ($P < 0.0001$), whereas single drug treatment with AE or AI was not statistically different from control. As shown in Fig. 2A, proliferation of LTLT-Ca cells was not inhibited with letrozole (10^{-12} to 10^{-5} mol/L), whereas cotreatment with trastuzumab (100 $\mu\text{g}/\text{mL}$) and letrozole inhibited the growth of LTLT-Ca cells in a dose-dependent manner. However, in MCF-7Ca cells, the combination of letrozole plus trastuzumab was not significantly different from letrozole at 10^{-9} to 10^{-5} mol/L but different from letrozole alone at 10^{-12} to 10^{-10} mol/L (Fig. 2B). Although the IC_{50} value of letrozole in the presence of trastuzumab was 2-log lower than that in the absence of trastuzumab, it should be noted that this effect was not seen *in vivo*.

The effect of combining trastuzumab plus letrozole was also examined in letrozole-refractory LTLT-Ca xenografts (data not

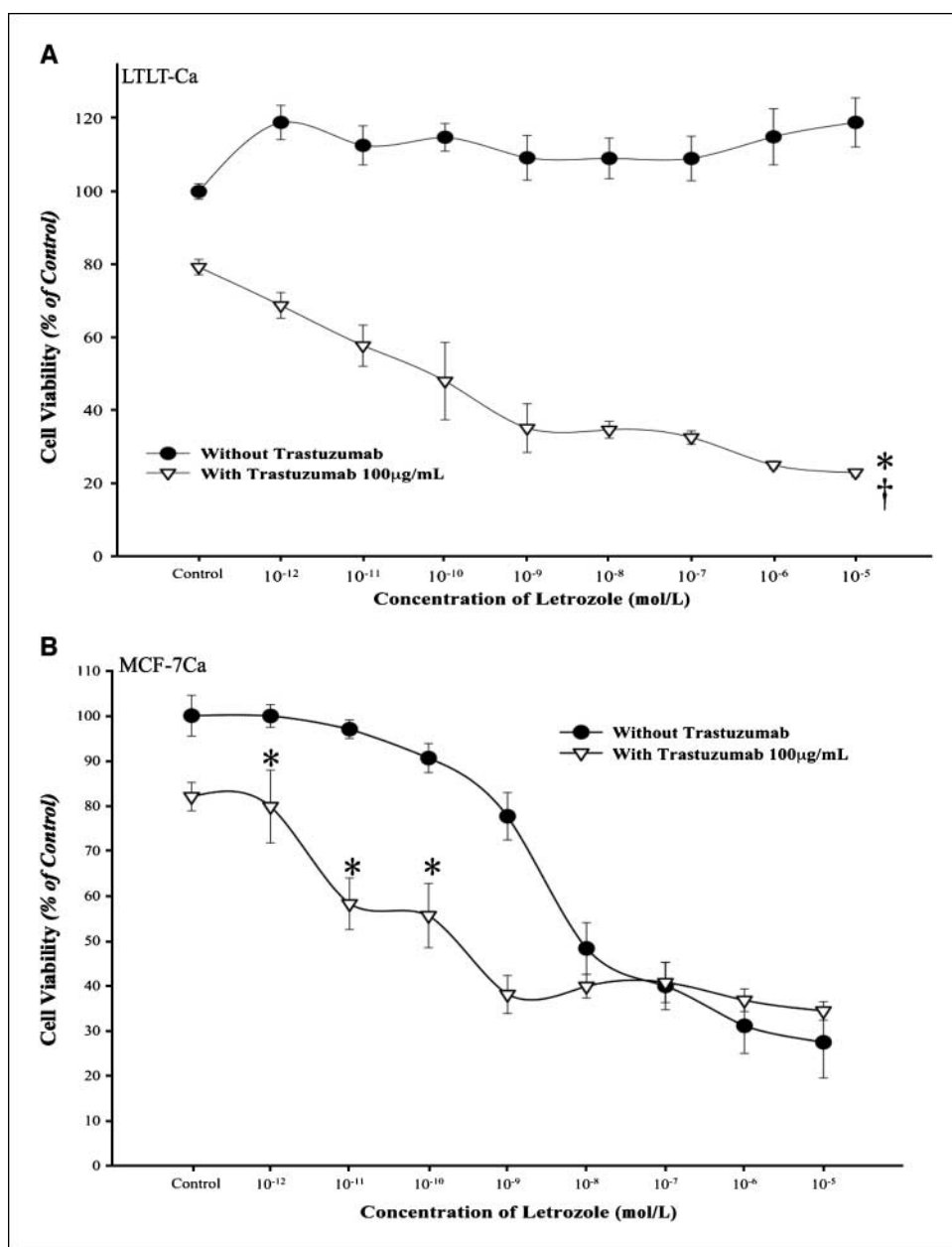


Figure 2. A, effect of combination of letrozole and trastuzumab in LTLT-Ca cells. Viability of cells was measured by MTT assay after 6-d treatment with letrozole (10^{-12} to 10^{-5} mol/L) alone or in the presence of trastuzumab (100 $\mu\text{g}/\text{mL}$) as described in Materials and Methods. The treatment with the combination of letrozole plus trastuzumab was significantly better than single drug treatment or control. *, $P < 0.01$ (10^{-12} to 10^{-9} mol/L); †, $P < 0.0001$ (10^{-8} to 10^{-5} mol/L). B, effect of combination of letrozole and trastuzumab in MCF-7Ca cells. Viability of cells was measured by MTT assay after 6-d treatment with letrozole (10^{-12} to 10^{-5} mol/L) alone or in the presence of trastuzumab (100 $\mu\text{g}/\text{mL}$) as described in Materials and Methods. Combination of letrozole plus trastuzumab was significantly better than single drug treatment or control. *, $P < 0.0001$ (10^{-12} to 10^{-10} mol/L).

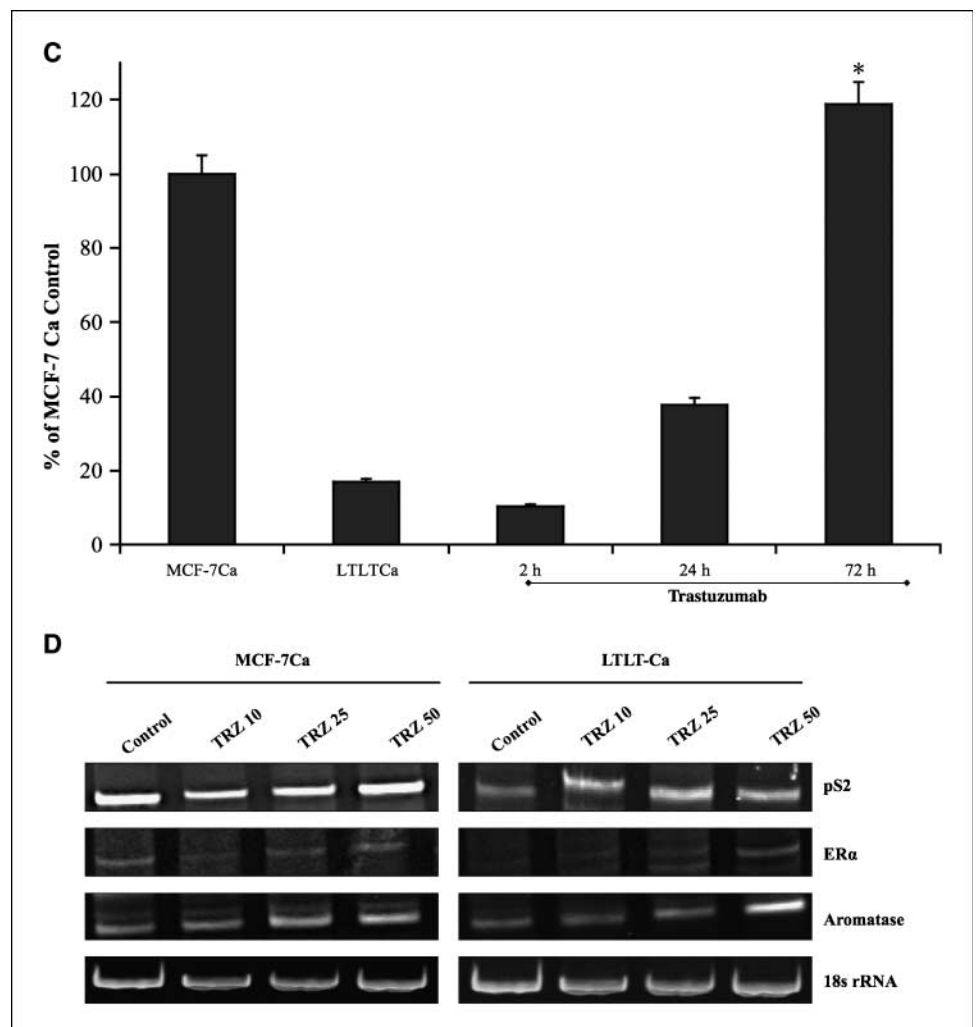
shown). The tumors of mice receiving trastuzumab plus letrozole regressed significantly in volume. The combination was significantly better than trastuzumab alone ($P < 0.0001$), letrozole alone ($P = 0.0001$), and control ($P < 0.0001$), although trastuzumab alone was significantly better than control ($P < 0.0001$). These data suggest that combining letrozole plus trastuzumab was significantly more effective than single agent in letrozole-refractory LTLT-Ca xenografts (26).

Trastuzumab up-regulated ER α - and E₂-mediated transcription in LTLT-Ca cells. Treatment with trastuzumab up-regulated ER α in LTLT-Ca cells (Fig. 1B). The maximum increase of ER α was seen at 24 hours and was found to be 0.83-fold compared with basal level of ER α in MCF-7Ca cells. A 10-fold higher level of ER α was found in LTLT-Ca cells compared with basal levels (0.83 compared with 0.08). In addition, trastuzumab pretreatment followed by E₂ treatment for 1 hour increased ER-mediated transcription in a time-dependent manner (Fig. 2C). A 72-hour pretreatment of LTLT-Ca cells with trastuzumab followed by 1 hour of E₂ treatment induced ER α transcriptional activation to the same extent as in parental MCF-7Ca cells stimulated with E₂ alone.

In vitro ChIP assay and reverse transcription-PCR (RT-PCR) analysis were performed to examine the effect of trastuzumab alone or in combination with E₂ on ER α -mediated transcription.

When stimulated with trastuzumab, MCF-7Ca and LTLT-Ca cells exhibit increased transcriptional activation as evidenced by increase in the expression of pS2 mRNA, a known ER α -responsive gene. This transcriptional activation was found to be dose dependent (Fig. 2D). In addition to pS2, the transcription of ER α and CYP-19 gene was found to be up-regulated in a dose-dependent manner. *In vitro* ChIP assay was performed to examine recruitment of ER α to the promoter region of pS2 and aromatase gene. The Western blotting for histone H3 confirms recruitment of ER α to the DNA and RNA polymerase II expression confirms transcriptional activation (Fig. 3A). As shown in Fig. 3B, E₂ treatment in MCF-7Ca cells induces recruitment of ER α to the pS2 promoter. Similarly, trastuzumab induced association of ER α to the pS2 promoter region. However, trastuzumab plus E₂ were not able to increase this association further. In LTLT-Ca cells, the basal level of promoter activity was not changed with E₂ or trastuzumab treatment. However, the combination of E₂ plus trastuzumab increased the recruitment of ER α to the pS2 promoter by 1.9-fold compared with the control. These results confirm that trastuzumab induces ER α -mediated transcription of downstream genes such as pS2. In addition, ER α was also recruited to the aromatase I.3/II promoter after treatment with trastuzumab, E₂, and the combination in LTLT-Ca cells. In MCF-7Ca cells, trastuzumab and E₂ increase recruitment of ER α to the aromatase I.3/II promoter;

Figure 2. Continued. C, effect of trastuzumab treatment on transactivation of ER α in LTLT-Ca cells. The ER α transactivation assay was performed as described in Materials and Methods. The treatment with trastuzumab increased ER α activation in a time-dependent manner. *, $P < 0.001$. D, effect of trastuzumab (TRZ) at various doses on the mRNA expression of ER α , pS2, and aromatase in MCF-7Ca and LTLT-Ca cells. Expression of mRNA was examined using RT-PCR as described in Materials and Methods. Blot shows ER α at 419 bp, pS2 at 245 bp, aromatase (CYP-19) at 293 bp, and 18s rRNA at 283 bp.



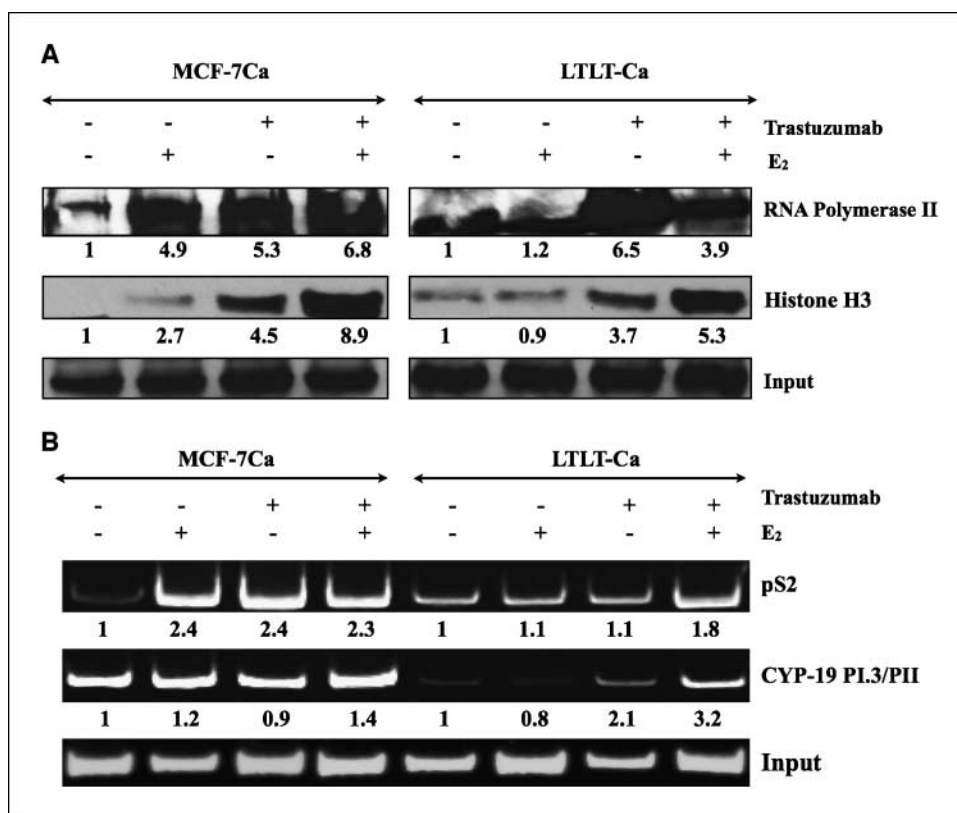


Figure 3. A, effect of trastuzumab and E₂ alone or in combination on the ER α -mediated transcriptional activation in MCF-7Ca and LTLT-Ca cells. The *in vitro* ChIP assay was performed as described in Materials and Methods. E₂-induced recruitment of ER α to the DNA and transcriptional activation in MCF-7Ca and LTLT-Ca cells was measured by Western blotting. The blot shows histone H3 at 15 kDa and RNA polymerase II at 300 kDa. *Left*, MCF-7Ca cells; *right*, LTLT-Ca cells. For both panels: *lane 1*, E₂W control; *lane 2*, E₂ (10 nmol/L); *lane 3*, trastuzumab (100 μ g/mL); *lane 4*, trastuzumab plus E₂. B, effect of trastuzumab and E₂ alone or in combination on the ER α -mediated transcriptional activation in MCF-7Ca and LTLT-Ca cells. The *in vitro* ChIP assay was performed as described earlier. E₂-induced recruitment of ER α to the aromatase 1.3/II and pS2 promoter in MCF-7Ca and LTLT-Ca cells was examined by PCR. The blot shows aromatase product at 317 bp and pS2 at 415 bp. Input indicates samples before immunoprecipitation. *Left*, MCF-7Ca cells; *right*, LTLT-Ca cells. For both panels: *lane 1*, E₂W control; *lane 2*, E₂ (10 nmol/L); *lane 3*, trastuzumab (100 μ g/mL); *lane 4*, trastuzumab plus E₂.

however, the combination did not increase this further. The MCF-7Ca cells may require different treatment period with trastuzumab to exhibit similar effect. These results suggest that trastuzumab activated the aromatase transcription in ER α -dependent manner in LTLT-Ca cells.

Trastuzumab amplified mitogenic effects of estradiol *in vitro* and *in vivo*. E₂ stimulation of MCF-7Ca cells resulted in a typical biphasic dose-response curve where maximum stimulation occurs at a concentration of $\sim 10^{-9}$ mol/L (Fig. 3C). In contrast, as reported in our earlier studies, proliferation of LTLT-Ca cells is not stimulated by E₂ (1, 27). However, when pretreated with trastuzumab (100 μ g/mL) for 72 hours, LTLT-Ca cells exhibited a marked stimulation of proliferation at concentrations of 10^{-12} to 10^{-7} mol/L when compared with E₂ alone ($P < 0.0001$). In addition, when MCF-7Ca cells were pretreated with trastuzumab, E₂-stimulated proliferation was increased at concentrations of 10^{-11} to 10^{-10} mol/L ($P = 0.02$ and 0.03 , respectively). The results suggest that inhibition of Her-2 restores ER α and E₂ sensitivity and that Her-2 is a negative regulator of ER.

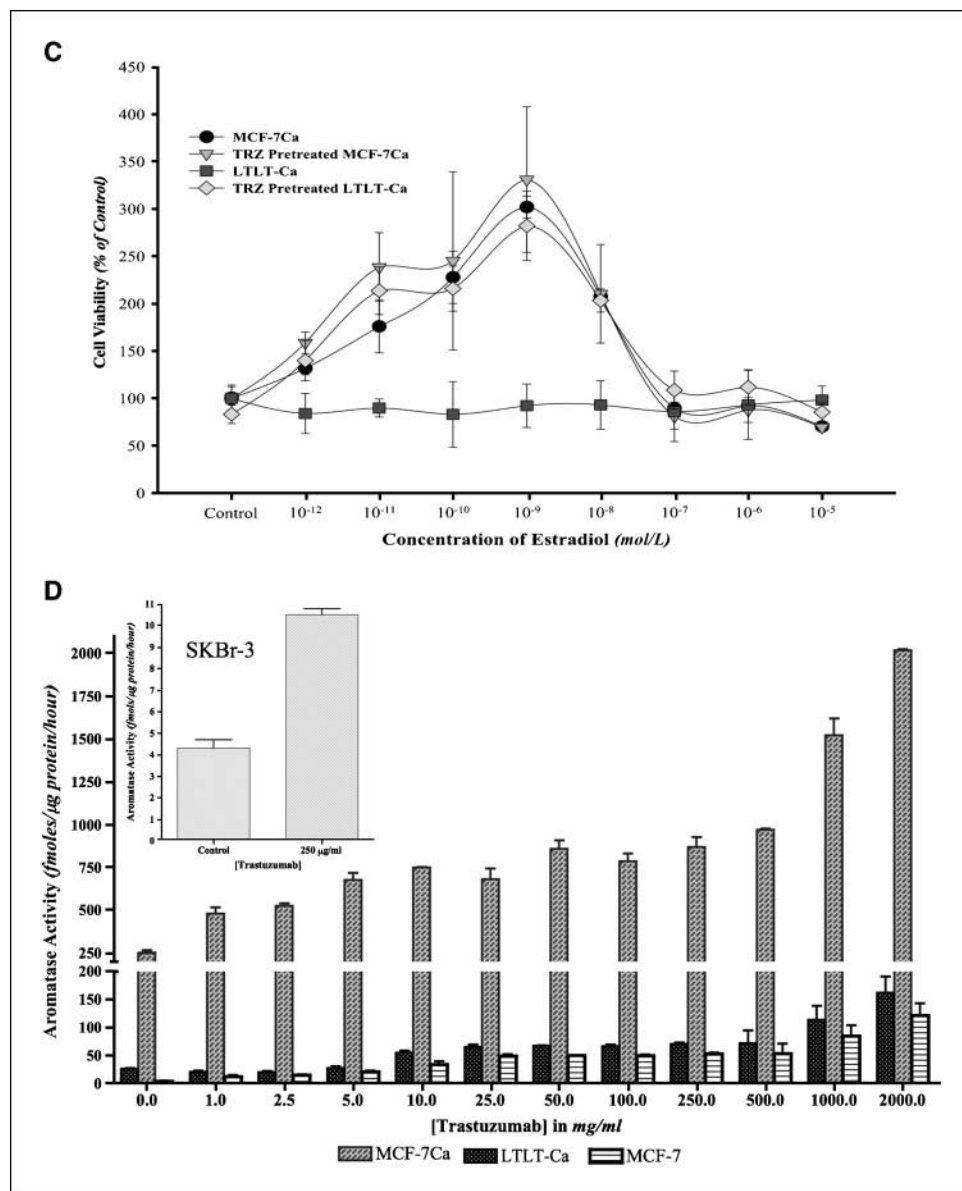
Pretreatment of MCF-7Ca, MCF-7, and LTLT-Ca cells with trastuzumab for 24 hours also increased aromatase activity in a dose-dependent manner (Fig. 3D). At the same time, aromatase protein expression was up-regulated by trastuzumab in a dose-dependent manner along with ER α (Fig. 4A). Trastuzumab caused an increase in the aromatase activity of MCF-7, suggesting that trastuzumab influences endogenous aromatase. To investigate whether suppressing Her-2 resulted in up-regulation of ER α and aromatase was limited to LTLT-Ca cells, we carried out the same experiment with ER-negative and Her-2-positive SKBr-3 cells. The results were similar, confirming that inhibition of Her-2 results in increased aromatase activity (Fig. 3D, *inset*) and ER α up-regulation

(data not shown). However, this effect was not seen in ER-negative and Her-2-negative MDA-MB-231 cells (data not shown). Trastuzumab did not bind competitively to ER α (Fig. 4B), suggesting that the stimulatory effects were ER α dependent, not due to intrinsic estrogenic properties of trastuzumab. In addition, when MCF-7Ca cells were cotreated with increasing doses of trastuzumab for 24 hours followed by 1 nmol/L E₂ for 1 hour, transcriptional activity of ER α was found to be up-regulated in a dose-dependent manner. This increase was found to be higher than E₂ (1 nmol/L) treatment alone (Fig. 4C).

The measurement of uterine weight is a useful bioassay that correlates with the levels of circulating estrogens in the body of the mice. The uteri of mice bearing LTLT-Ca xenografts treated with trastuzumab were removed and weighed at the completion of the experiment. Trastuzumab induced a statistically significant ($P = 0.001$) dose-dependent increase in uterine wet weight compared with controls (Fig. 4D). Increased uterine weight suggests that cotreatment with trastuzumab acts to enhance ER α and effects of E₂ on the uterus. Furthermore, increased tumor aromatase activity suggests that trastuzumab increases E₂ synthesis from Δ^4 A (data not shown).

Trastuzumab is ineffective in inhibiting growth of MCF-7Ca tumors. MCF-7Ca xenografts were grown in female ovariectomized mice. When tumors reached measurable size ~ 300 mm³, mice were assigned to four groups: (a) control ($n = 5$); (b) trastuzumab, 5 mg/kg/wk, divided in two doses ($n = 5$); (c) letrozole, 10 μ g/d, plus trastuzumab, 5 mg/kg/wk, divided in two doses ($n = 5$); and (d) letrozole, 10 μ g/d ($n = 30$). The tumors were measured weekly and volume was calculated as described in Materials and Methods. Trastuzumab did not inhibit the growth of MCF-7Ca tumors (Fig. 5A). The growth rate

Figure 3. Continued. C, effect of estradiol on proliferation of MCF-7Ca and LTLT-Ca cells in the presence or absence of trastuzumab before treatment. Viability of cells was measured by MTT assay after 6-d treatment with E_2 (10^{-12} to 10^{-5} mol/L) alone or in the presence of trastuzumab (100 μ g/mL). When pretreated with trastuzumab (100 μ g/mL), LTLT-Ca cells exhibit a significantly marked stimulation of proliferation in response to E_2 at concentrations of 10^{-12} to 10^{-7} mol/L when compared with E_2 alone ($P < 0.0001$). When MCF-7Ca cells were pretreated with trastuzumab, E_2 -stimulated proliferation was increased at concentrations 10^{-11} to 10^{-10} mol/L ($P = 0.02$ and 0.03 , respectively). D, effect of trastuzumab treatment at various doses on aromatase activity of MCF-7, MCF-7Ca, and LTLT-Ca cells. MCF-7, MCF-7Ca, and LTLT-Ca cells were treated with trastuzumab at varying doses for 24 h and then incubated with [3 H]androstenedione for 18 h. The activity of the enzyme after treatment is corrected for total protein amount after treatment. Inset, effect of trastuzumab treatment at 250 μ g/mL on aromatase activity of SKBr-3 cells. SKBr-3 cells were treated with trastuzumab at 250 μ g/mL for 24 h and then incubated with [3 H]androstenedione for 18 h. The activity of the enzyme after treatment is corrected for total protein amount after treatment.



of control tumors (Δ^4A , 100 μ g/d) was $\beta i = 0.17 \pm 0.1$, which was not statistically different from that of tumors in mice treated with trastuzumab ($\beta i = 0.19 \pm 0.14$) over the first 7 weeks. The mice in both these groups (control and trastuzumab) were sacrificed at week 7 due to large tumor volume. The tumors and uteri of the treated mice were removed, weighed, and stored at -80°C for any additional analysis. The tumor weights (Fig. 5B) of control (1.37 ± 0.57 g) and trastuzumab (2.68 ± 0.57 g) were not statistically different ($P = 0.14$). However, trastuzumab treatment alone was significantly less effective than other treatments [versus letrozole ($P = 0.0009$) or versus trastuzumab plus letrozole ($P = 0.0001$)].

As shown in Fig. 5C, uteri in mice treated with trastuzumab weighed significantly more than those treated with Δ^4A ($P = 0.008$). The increase in uterine weight again suggests amplified growth-stimulatory effects of E_2 on cotreatment with trastuzumab.

Combination of trastuzumab plus letrozole is more effective than either drug alone in letrozole-refractory tumors. As

shown in Fig. 5A, combination of letrozole plus trastuzumab was effective in reducing the tumor growth rate ($\beta i = -0.04 \pm 0.04$ over weeks 0–15; $\beta i = 0.28 \pm 0.06$ over weeks 15–27). However, the combination was no more effective than letrozole as single agent ($\beta i = -0.01 \pm 0.02$ over weeks 0–15; $\beta i = 0.1 \pm 0.08$ over weeks 15–27).

Letrozole inhibited the growth of these tumors for a prolonged period (13 weeks). Nevertheless, tumors ultimately began to grow on continued treatment and had doubled in volume by week 15. At this time, the mice were subdivided into three groups: (a) trastuzumab, 5 mg/kg/wk (two doses; $n = 10$); (b) letrozole, 10 μ g/d, plus trastuzumab, 5 mg/kg/wk ($n = 10$); and (c) letrozole, 10 μ g/d ($n = 10$). The experiment was terminated on week 28. Tumors in mice switched to combination therapy following letrozole resistance responded better than combination treatment from week 0 ($P < 0.0001$). This suggests that on letrozole resistance, the addition of trastuzumab to the treatment regimen is superior to combination therapy from the

beginning. The growth rate of these tumors was significantly different from the tumors of mice that stayed on letrozole treatment ($P = 0.008$). Tumors treated with letrozole responded better when switched to letrozole plus trastuzumab than those kept on letrozole. Letrozole-refractory tumors switched to trastuzumab alone responded to the treatment only for the first 3 weeks (weeks 16–19) but then began to regrow at the rate similar to that of the letrozole-treated mice (weeks 15–28; $P = 0.97$). Thus, on resistance to letrozole, the addition of trastuzumab was more effective than the switch to trastuzumab, suggesting that Her-2 inhibition extends sensitivity of letrozole.

Protein expression and activity of tumors treated with letrozole and trastuzumab alone or in combination. At 28 weeks (Fig. 5A), tumors of mice bearing MCF-7Ca xenografts were analyzed for expression of Her-2, p-MAPK, MAPK, aromatase, and ER α protein expression by Western blotting

(Fig. 5D). Treatment with trastuzumab increased ER α and decreased Her-2 and p-MAPK protein expression. In contrast, letrozole reduced ER α and increased Her-2 and p-MAPK levels. The combination of letrozole plus trastuzumab did not affect ER α levels and caused moderate increases in Her-2 and p-MAPK. The tumors of mice switched from letrozole to trastuzumab showed up-regulation of ER and down-regulation of Her-2 and p-MAPK compared with letrozole. This would be consistent with stimulation of growth due to release from aromatase inhibition, allowing estrogen production. In mice treated with letrozole and the addition of trastuzumab on tumor volume doubling, ER α levels were moderately increased, p-MAPK was down-regulated, and Her-2 was moderately reduced.

As shown in Fig. 6A, trastuzumab increased aromatase activity in the tumors, whereas letrozole inhibited aromatase activity. This increased activity was also accompanied by a 3.7-fold up-regulation

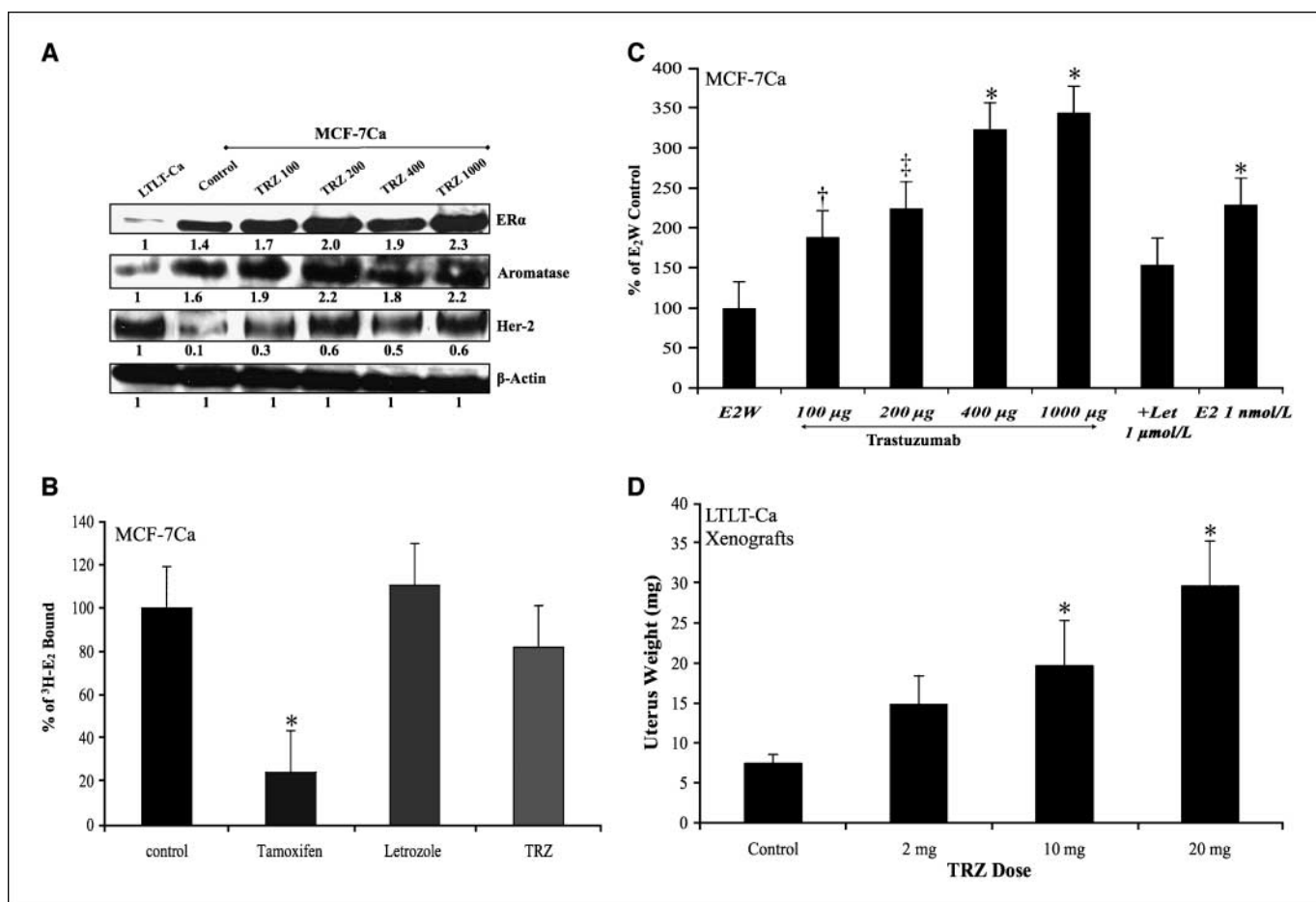
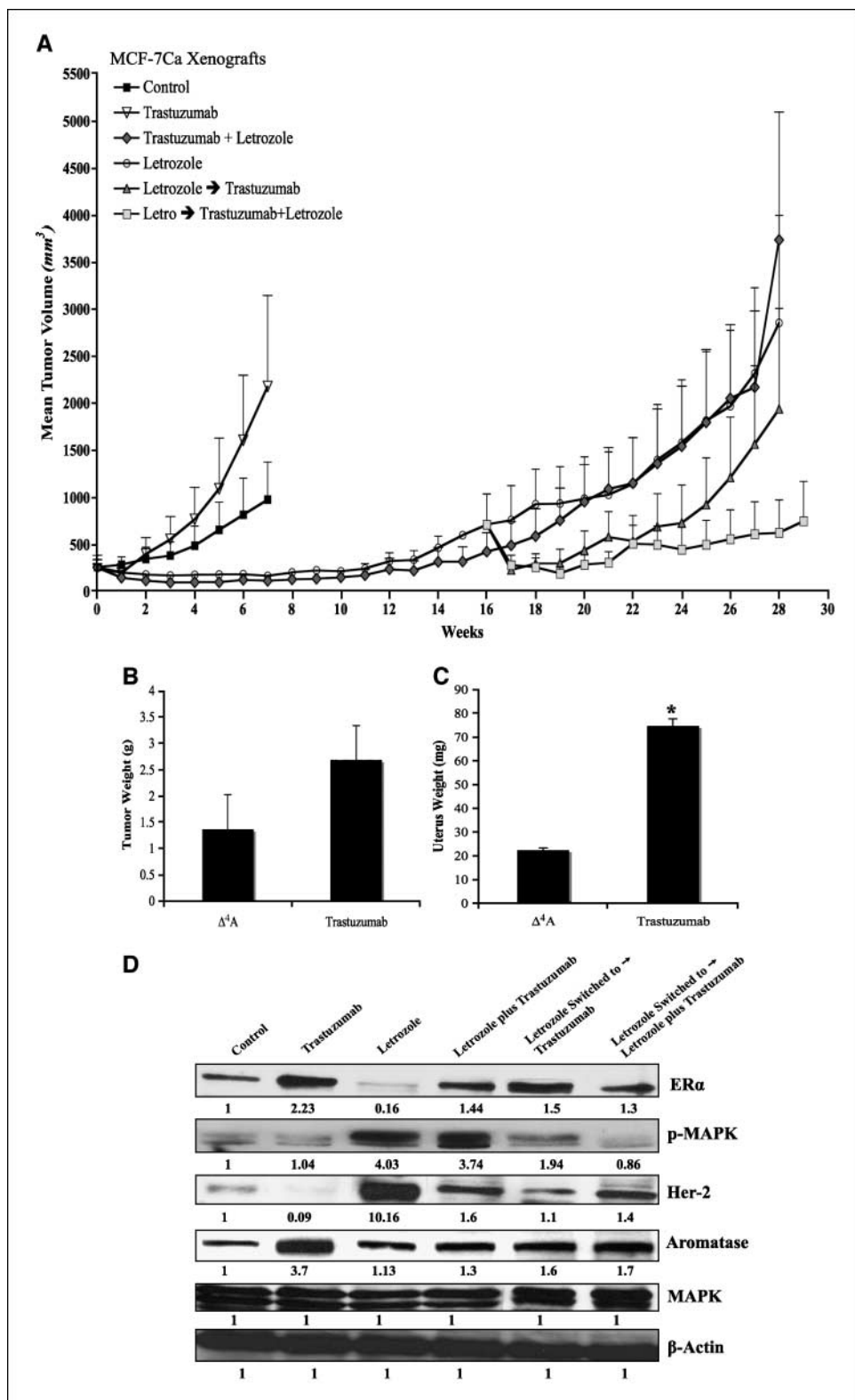


Figure 4. A, effect of trastuzumab treatment at various concentrations on protein expression of ER α , Her-2, and CYP-19 in MCF-7Ca cells. Expression of proteins was examined using Western immunoblotting as described in Materials and Methods. Blot shows ER α at 66 kDa, CYP-19 at 55 kDa, Her-2 at 185 kDa, and β -actin at 45 kDa. The blots show a single representative of three independent experiments. The blots were stripped and reprobed for β -actin to verify equal loading. B, effect of trastuzumab treatment on binding affinity of estradiol to ER α in MCF-7Ca cells. The competitive binding study was performed as described in Materials and Methods. The difference between trastuzumab and control in the percent of radioactive estradiol bound to ER α was 18.053, which was not statistically significant ($P = 0.4$, using Kruskal-Wallis test and Dunn's multiple comparison). C, effect of trastuzumab treatment at various doses on transactivation of ER α in MCF-7Ca cells. The ER α transactivation assay was performed to measure transcriptional activation of ER α in MCF-7Ca cells, as described in Materials and Methods. The treatment with trastuzumab increased ER α activation in a dose-dependent manner. The differences between E $_2$ W control and trastuzumab treatment (100, 200, 400, and 1,000 μ g/mL) were -111.31 (\dagger , $P = 0.06$), -156.23 (\dagger , $P < 0.01$), -279.91 ($*$, $P < 0.001$), and -305.45 ($*$, $P < 0.001$) and 0.04 for E $_2$. When combined with 1 μ mol/L letrozole, 1,000 μ g/mL trastuzumab did not stimulate ER α activation. Letrozole treatment was not significantly different from the E $_2$ W control. One-way ANOVA with post-hoc Tukey-Kramer test ($*$, $P < 0.05$). D, effect of trastuzumab treatment at various doses on uterine wet weight of mice bearing LTLT-Ca xenografts. The mice bearing LTLT-Ca xenografts were treated with trastuzumab at varying doses for 12 wk, after which the uteri were removed and weighed. The mice in control group had a mean uterine weight of 6.4 ± 2.2 mg, which was the lowest uterine weight (exact two-sided $P = 0.008$ by the Wilcoxon test) and significantly lower than in mice treated with 2, 10, and 20 mg of trastuzumab. The mean uterine wet weights ranged from 15.4 ± 2.2 mg to 20.4 ± 2.2 mg to 29.8 ± 2.2 mg.

Figure 5. A, effect of trastuzumab alone or in combination with letrozole on the growth of MCF-7Ca xenografts.

Trastuzumab (5 mg/kg/wk) did not inhibit the growth of MCF-7Ca tumors. The difference in the exponential variable governing growth rate of control versus trastuzumab treatment was 0.02 ± 0.14 , which was not statistically significant ($P = 0.86$). The difference in the exponential variable governing growth rate of trastuzumab plus letrozole versus letrozole was 0.49 ($P = 0.0001$). The difference in the exponential variable governing growth rate of trastuzumab versus letrozole was 0.32 ($P = 0.0009$). The difference in the exponential variable governing growth rate of letrozole versus letrozole switched to letrozole plus trastuzumab was 0.21 ± 0.08 ($P = 0.008$). The difference in the exponential variable governing growth rate of letrozole plus trastuzumab versus letrozole switched to letrozole plus trastuzumab was 0.39 ± 0.09 ($P < 0.0001$). The difference in the exponential variable governing rate of letrozole switched to trastuzumab versus letrozole switched to trastuzumab plus trastuzumab was 0.2 ± 0.08 ($P = 0.011$) over weeks 15 to 28. When compared with week 29, the difference in the exponential variable governing growth rate of letrozole versus letrozole switched to trastuzumab was 0.005 ± 0.08 ($P = 0.97$). B, effect of trastuzumab on the tumor weight of the mice bearing MCF-7Ca xenografts. The mean tumor weight of trastuzumab-treated mice was 2.68 ± 0.57 g, which was not significantly different from those of the Δ^4A -treated mice (1.37 ± 0.57 g; $P = 0.14$). The tumor weights of other groups are not compared due to difference in the time of termination. C, effect of trastuzumab on the uterine wet weight of mice bearing MCF-7Ca xenografts. The average weight of the atrophic uterus in ovariectomized mice is ~ 10 mg; the greater uterine weight of mice receiving Δ^4A (22.42 ± 0.92 mg) indicates that aromatase in the tumors is producing enough estrogens to maintain the uterine weight similar to intact mice in diestrus. When mice were treated with trastuzumab, the uteri weighed significantly more (74.8 ± 0.92 mg) than Δ^4A -treated mice (Wilcoxon rank sum test, two-sided exact $P = 0.008$). The uterus weights of other groups are not compared due to difference in the time of termination. D, effect of trastuzumab and letrozole alone or in combination on protein expression of ER α , Her-2, MAPK, and CYP-19 in MCF-7Ca xenografts. Expression of proteins was examined using Western immunoblotting as described in Materials and Methods. Blot shows ER α at 66 kDa, Her-2 at 185 kDa, p-MAPK and MAPK at 42 to 44 kDa, CYP-19 at 55 kDa, and β -actin at 45 kDa. The blots show a single representative of three independent experiments. The blots were stripped and reprobbed for β -actin to verify equal loading.



of aromatase protein expression (Fig. 5D). The aromatase activity in the tumor samples from letrozole, letrozole plus trastuzumab, and letrozole switched to letrozole plus trastuzumab was found to be significantly lower than control ($P < 0.001$) or trastuzumab treatment ($P < 0.001$). The aromatase activity of tumors from

letrozole switched to trastuzumab alone-treated mice was, however, not significantly different from control but significantly higher than letrozole alone ($P < 0.01$). However, aromatase protein expression in all these groups was not significantly different from control. The data suggest that letrozole maintains aromatase

inhibition after prolonged treatment and switching to trastuzumab therapy removes the inhibitory effect of the AI on aromatase. Furthermore, tumors of mice treated with letrozole switched to letrozole plus trastuzumab show reduced aromatase activity,

suggesting that addition of trastuzumab to letrozole did not interfere directly with aromatase inhibition by letrozole.

Trastuzumab increases transcriptional activation of ER α in MCF-7Ca xenografts. The *in vivo* ChIP assay was used to

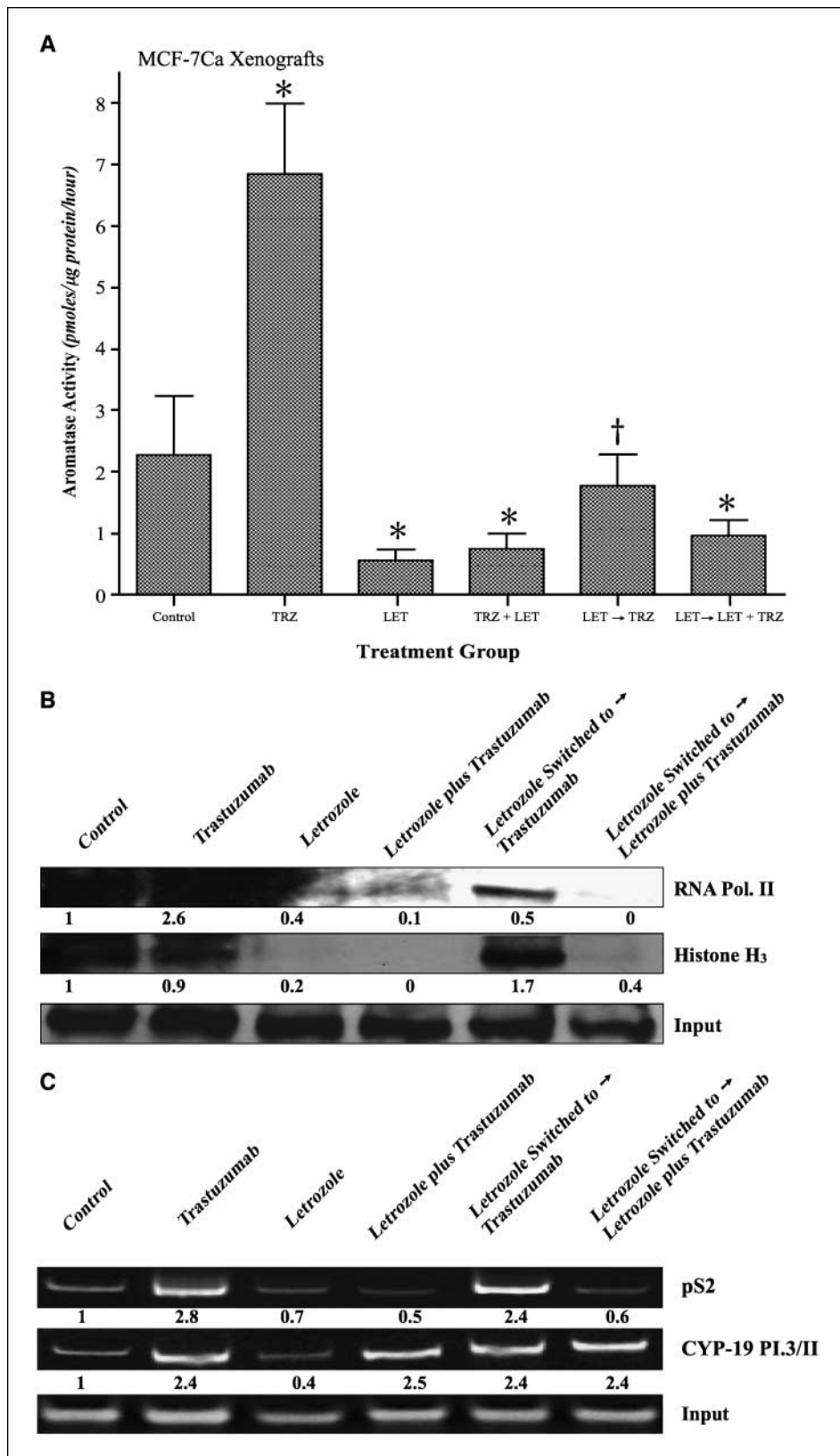


Figure 6. A, effect of trastuzumab and letrozole alone or in combination on aromatase activity of MCF-7Ca xenografts. The tumors of mice treated with letrozole, trastuzumab, and the combinations were examined for aromatase activity as described in Materials and Methods. The activity of the enzyme after treatment is corrected for total protein amount in the tumors. Aromatase activity of MCF-7Ca xenografts treated with trastuzumab is significantly higher than control (*, $P < 0.001$). Aromatase activity of control is significantly higher compared with letrozole ($P < 0.001$), letrozole plus trastuzumab (*, $P < 0.001$), and letrozole switched to letrozole plus trastuzumab (*, $P < 0.001$). The aromatase activity of letrozole switched to trastuzumab was not significantly different from Δ^4 A-treated control but significantly higher than letrozole (\dagger , $P < 0.01$). One-way ANOVA, Tukey-Kramer multiple comparisons test. B, effect of trastuzumab and letrozole alone or in combination on the ER α -mediated transcriptional activation in MCF-7Ca xenografts. The *in vivo* ChIP assay was performed as described in Materials and Methods. E₂-induced recruitment of ER α to the DNA in MCF-7Ca xenografts. The blot shows histone H3 at 15 kDa and RNA polymerase II at 300 kDa. ChIP analysis was done using ER α antibody. Input indicates samples before immunoprecipitation. C, effect of trastuzumab and letrozole alone or in combination on the ER α -mediated transcriptional activation in MCF-7Ca xenografts. The *in vivo* ChIP assay was performed as described earlier. Treatment-induced recruitment of ER α to the aromatase 1.3/II and pS2 promoter in MCF-7Ca xenografts was examined by PCR. Input indicates samples before immunoprecipitation. The blot shows aromatase product at 317 bp and pS2 at 415 bp.

measure the effect of trastuzumab on transcriptional activation of ER α in MCF-7Ca xenografts. Δ^4 A-treated control and trastuzumab-treated tumors exhibited active transcription of ER α , as evidenced by recruitment of histone H3 and RNA polymerase II into the transcriptional complex (Fig. 6B). The treatment of MCF-7Ca tumors with trastuzumab increased recruitment of ER α to the pS2 and aromatase I.3/II promoter (Fig. 6C). These findings support *in vivo* tumor volume data and suggest that trastuzumab treatment in a hormone-sensitive breast cancer model is agonistic via its effects on Her-2 and hence the ER. As such, Her-2 inhibition without blockade of estrogen signaling in the clinical setting could be detrimental.

Discussion

Although AI letrozole is more effective and tumor growth is suppressed over an extended period compared with tamoxifen, eventually tumors become resistant to AI therapy (1). Previous results indicate that tumor growth is maintained by activating Her-2/MAPK signaling pathways in letrozole-resistant LTLT-Ca cells and letrozole-refractory tumors. In addition, ER expression is decreased and cells become insensitive to E₂, suggesting a hormone-refractory phenotype. Our previous studies also indicated that the combination of letrozole with MAPK inhibitor PD98059 up-regulated ER α expression, consistent with the reports that hyperactivation of MAPK induces loss of ER α in breast cancer cells (1, 28). Her-2 is overexpressed in about 25% to 30% of breast cancers and correlates with poor disease-free survival and overall survival (29, 30). With the development of trastuzumab, effective targeted treatment of Her-2-overexpressing cancers has been possible. Treatment with trastuzumab also resulted in up-regulation of ER α . We have shown that loss of ER α expression induced by MAPK hyperactivation is reversible as observed in findings of others (31). Our studies show that trastuzumab by blocking Her-2 can reverse the suppression of ER α . To prevent development of letrozole resistance and restore hormone sensitivity of resistant cells, we used trastuzumab to inhibit the Her-2/MAPK pathway in the present study.

The combination of trastuzumab with letrozole reversed resistance to the AI and restored responsiveness of the tumors. However, this effect was limited to letrozole-refractory and Her-2-overexpressing cells and tumors. Trastuzumab alone was only effective for a brief period of 4 weeks in letrozole-refractory tumors. In the tumors with low Her-2 levels, the letrozole plus trastuzumab combination was no more effective than letrozole single agent. However, in Her-2-overexpressing tumors, trastuzumab plus letrozole was far superior in inhibiting tumor growth compared with either single agent (Fig. 5A). These results suggest that trastuzumab restores sensitivity of LTLT-Ca cells to letrozole by inhibiting Her-2 and up-regulation of ER α . As such, blockade of the ER α pathway remains an essential component of tumor and cell growth inhibition. Up-regulation of intratumoral aromatase was also seen with trastuzumab treatment to make the cells more responsive to AIs.

In our current study, we have shown that inhibition of Her-2 with trastuzumab results in activation of ER α -mediated signaling pathway. Based on these data, we hypothesize that an inverse and compensatory relationship exists between Her-2 and ER α and inhibition of one pathway leads to activation of the other.

Several reports have suggested that translocation of ER α to the membrane may be responsible for the cross-talk with EGFR family members in endocrine-resistant phenotype (32–34), whereas a few reports have also suggested that EGFR family transmembrane receptors such as Her-2 can translocate to the nucleus and act as transcription factors (35–38).

Studies performed in trastuzumab-resistant variants of breast cancer cell lines have indicated up-regulation of transforming growth factor α (TGF α) and vascular endothelial growth factor (VEGF; refs. 39, 40). Interestingly, both VEGF and TGF α are estrogen-responsive genes (41). These data are consistent with our results and suggest that Her-2 suppresses ER α , as resistance to trastuzumab is associated with up-regulation of ER α -responsive genes (39, 40). Our studies show that trastuzumab alone was not an effective treatment strategy in this model and the data suggest that it is likely to be due to up-regulation of intratumoral aromatase and ER α . To distinguish whether up-regulation of ER α was a result of increased protein synthesis or reduced degradation, cells were treated with trastuzumab in the presence or absence of cycloheximide (translational inhibitor). Western immunoblotting analysis revealed that trastuzumab treatment increased ER α to a greater extent in the absence of cycloheximide, suggesting that trastuzumab modulates protein synthesis. However, even in the presence of cycloheximide, ER α protein was up-regulated by trastuzumab treatment, suggesting that trastuzumab treatment affects protein degradation as well (data not shown). In addition, RT-PCR analysis revealed that ER α mRNA expression is increased with trastuzumab treatment in a dose-dependent manner (Fig. 2D).

In agreement with our findings, clinical studies have shown that trastuzumab as single agent has promising effects in first-line treatment of ~40% breast cancer patients (42). However, the median duration of response is only ~8 months. Furthermore, intrinsic or *de novo* resistance to trastuzumab in Her-2-overexpressing breast cancers has been reported. As the use of trastuzumab is now extended to adjuvant treatment of breast cancer, it is important to assess the molecular effects of trastuzumab on Her-2-overexpressing breast cancer cells and determine appropriate strategies for optimal treatment. Our studies clearly show the importance of inhibiting both estrogen signaling by AI letrozole and the growth factor receptor Her-2 pathway in overcoming resistance to therapy. However, if used for treatment of hormone-responsive tumors, trastuzumab may amplify estrogen signaling and stimulate tumor growth. The results indicate that inhibition of Her-2 via trastuzumab can restore the responsiveness of tumors to letrozole and trastuzumab, thus extending the use of AIs and delaying the need for chemotherapy.

Disclosure of Potential Conflicts of Interest

No potential conflicts of interest were disclosed.

Acknowledgments

Received 3/5/2008; revised 9/23/2008; accepted 11/4/2008; published OnlineFirst 02/03/2009.

Grant support: National Cancer Institute, NIH, grant CA-62483 (A. Brodie).

The costs of publication of this article were defrayed in part by the payment of page charges. This article must therefore be hereby marked *advertisement* in accordance with 18 U.S.C. Section 1734 solely to indicate this fact.

We thank Dr. Armina Kazi for her help with the RT-PCR and ChIP assays.

References

1. Jelovac D, Sabinis G, Long BJ, et al. Activation of mitogen-activated protein kinase in xenografts and cells during prolonged treatment with aromatase inhibitor letrozole. *Cancer Res* 2005;65:5380–9.
2. Long BJ, Jelovac D, Handratta V, et al. Therapeutic strategies using the aromatase inhibitor letrozole and tamoxifen in a breast cancer model. *J Natl Cancer Inst* 2004;96:456–65.
3. Long BJ, Jelovac D, Thiantanawat A, Brodie AM. The effect of second-line antiestrogen therapy on breast tumor growth after first-line treatment with the aromatase inhibitor letrozole: long-term studies using the intratumoral aromatase postmenopausal breast cancer model. *Clin Cancer Res* 2002;8:2378–88.
4. Sabinis GJ, Jelovac D, Long B, Brodie A. The role of growth factor receptor pathways in human breast cancer cells adapted to long-term estrogen deprivation. *Cancer Res* 2005;65:3903–10.
5. Shim WS, Conaway M, Masamura S, et al. Estradiol hypersensitivity and mitogen-activated protein kinase expression in long-term estrogen deprived human breast cancer cells *in vivo*. *Endocrinology* 2000;141:396–405.
6. Yue W, Wang JP, Conaway MR, Li Y, Santen RJ. Adaptive hypersensitivity following long-term estrogen deprivation: involvement of multiple signal pathways. *J Steroid Biochem Mol Biol* 2003;86:265–74.
7. Martin LA, Farmer I, Johnston SR, et al. Enhanced estrogen receptor (ER) α , ERBB2, and MAPK signal transduction pathways operate during the adaptation of MCF-7 cells to long term estrogen deprivation. *J Biol Chem* 2003;278:30458–68.
8. Shin I, Miller T, Arteaga CL. ErbB receptor signaling and therapeutic resistance to aromatase inhibitors. *Clin Cancer Res* 2006;12:1008–12s.
9. Shou J, Massarweh S, Osborne CK, et al. Mechanisms of tamoxifen resistance: increased estrogen receptor-HER2/neu cross-talk in ER/HER2-positive breast cancer. *J Natl Cancer Inst* 2004;96:926–35.
10. Johnston SR. Clinical efforts to combine endocrine agents with targeted therapies against epidermal growth factor receptor/human epidermal growth factor receptor 2 and mammalian target of rapamycin in breast cancer. *Clin Cancer Res* 2006;12:1061–8s.
11. Johnston SR. Combinations of endocrine and biological agents: present status of therapeutic and presurgical investigations. *Clin Cancer Res* 2005;11:889–99s.
12. Johnston SR. Clinical trials of intracellular signal transductions inhibitors for breast cancer—a strategy to overcome endocrine resistance. *Endocr Relat Cancer* 2005;12 Suppl 1:S145–57.
13. Kurokawa H, Arteaga CL. Inhibition of erbB receptor (HER) tyrosine kinases as a strategy to abrogate antiestrogen resistance in human breast cancer. *Clin Cancer Res* 2001;7:4436–42s; discussion 4411–12s.
14. Brodie A, Jelovac D, Macedo L, et al. Therapeutic observations in MCF-7 aromatase xenografts. *Clin Cancer Res* 2005;11:884–8s.
15. Brodie A, Jelovac D, Sabinis G, et al. Model systems: mechanisms involved in the loss of sensitivity to letrozole. *J Steroid Biochem Mol Biol* 2005;95:41–8.
16. Yue W, Brodie A. MCF-7 human breast carcinomas in nude mice as a model for evaluating aromatase inhibitors. *J Steroid Biochem Mol Biol* 1993;44:671–3.
17. Yue W, Zhou D, Chen S, Brodie A. A new nude mouse model for postmenopausal breast cancer using MCF-7 cells transfected with the human aromatase gene. *Cancer Res* 1994;54:5092–5.
18. Sabinis G, Goloubeva O, Jelovac D, Schayowitz A, Brodie A. Inhibition of the phosphatidylinositol 3-kinase/Akt pathway improves response of long-term estrogen-deprived breast cancer xenografts to antiestrogens. *Clin Cancer Res* 2007;13:2751–7.
19. Long BJ, Tilghman SL, Yue W, et al. The steroidal antiestrogen ICI 182,780 is an inhibitor of cellular aromatase activity. *J Steroid Biochem Mol Biol* 1998;67:293–304.
20. Kazi AA, Jones JM, Koos RD. Chromatin immunoprecipitation analysis of gene expression in the rat uterus *in vivo*: estrogen-induced recruitment of both estrogen receptor α and hypoxia-inducible factor 1 to the vascular endothelial growth factor promoter. *Mol Endocrinology* 2005;19:2006–19.
21. Saegusa M, Hashimura M, Hara A, Okayasu I. Up-regulation of pS2 expression during the development of adenocarcinomas but not squamous cell carcinomas of the uterine cervix, independently of expression of c-jun or oestrogen and progesterone receptors. *J Pathol* 2000;190:554–63.
22. Nakamura J, Lu Q, Aberdeen G, Albrecht E, Brodie A. The effect of estrogen on aromatase and vascular endothelial growth factor messenger ribonucleic acid in the normal nonhuman primate mammary gland. *J Clin Endocrinol Metab* 1999;84:1432–7.
23. Deb S, Zhou J, Amin SA, et al. A novel role of sodium butyrate in the regulation of cancer-associated aromatase promoters L3 and II by disrupting a transcriptional complex in breast adipose fibroblasts. *J Biol Chem* 2006;281:2585–97.
24. Zhou C, Zhou D, Esteban J, et al. Aromatase gene expression and its exon I usage in human breast tumors. Detection of aromatase messenger RNA by reverse transcription-polymerase chain reaction. *J Steroid Biochem Mol Biol* 1996;59:163–71.
25. Sebastian S, Bulun SE. A highly complex organization of the regulatory region of the human CYP19 (aromatase) gene revealed by the Human Genome Project. *J Clin Endocrinol Metab* 2001;86:4600–2.
26. Brodie A, Sabinis G, Macedo L. Xenograft models for aromatase inhibitor studies. *J Steroid Biochem Mol Biol* 2007;106:119–24.
27. Sabinis GJ, Schayowitz A, Goloubeva O, Brodie AMH. Trastuzumab increases sensitivity of hormone dependent and hormone refractory breast cancer cells to endocrine agents [abstract 991]. *Am Assoc Cancer Res Meet Abstr* 2007.
28. Oh AS, Lorant LA, Holloway JN, et al. Hyperactivation of MAPK induces loss of ER α expression in breast cancer cells. *Mol Endocrinology* 2001;15:1344–59.
29. Piccart M, Lohrisch C, Di Leo A, Larsimont D. The predictive value of HER2 in breast cancer. *Oncology* 2001;61 Suppl 2:73–82.
30. Slamon DJ, Clark GM, Wong SG, et al. Human breast cancer: correlation of relapse and survival with amplification of the HER-2/neu oncogene. *Science* 1987;235:177–82.
31. Creighton CJ, Hilger AM, Murthy S, et al. Activation of mitogen-activated protein kinase in estrogen receptor α -positive breast cancer cells *in vitro* induces an *in vivo* molecular phenotype of estrogen receptor α -negative human breast tumors. *Cancer Res* 2006;66:3903–11.
32. Levin ER, Pietras RJ. Estrogen receptors outside the nucleus in breast cancer. *Breast Cancer Res Treat* 2008;108:351–61.
33. Santen RJ, Song RX, McPherson R, et al. The role of mitogen-activated protein kinase in breast cancer. *J Steroid Biochem Mol Biol* 2002;80:239–56.
34. Song RX, Fan P, Yue W, Chen Y, Santen RJ. Role of receptor complexes in the extranuclear actions of estrogen receptor α in breast cancer. *Endocr Relat Cancer* 2006;13 Suppl 1:S3–13.
35. Hsu SC, Hung MC. Characterization of a novel tripartite nuclear localization sequence in the EGFR family. *J Biol Chem* 2007;282:10432–40.
36. Lo HW, Hsu SC, Hung MC. EGFR signaling pathway in breast cancers: from traditional signal transduction to direct nuclear translocalization. *Breast Cancer Res Treat* 2006;95:211–8.
37. Lo HW, Hung MC. Nuclear EGFR signalling network in cancers: linking EGFR pathway to cell cycle progression, nitric oxide pathway and patient survival. *Br J Cancer* 2007;96 Suppl:R16–20.
38. Xie Y, Hung MC. Nuclear localization of p185neu tyrosine kinase and its association with transcriptional transactivation. *Biochem Biophys Res Commun* 1994;203:1589–98.
39. du Manoir JM, Francia G, Man S, et al. Strategies for delaying or treating *in vivo* acquired resistance to trastuzumab in human breast cancer xenografts. *Clin Cancer Res* 2006;12:904–16.
40. Valabrega G, Montemurro F, Aglietta M. Trastuzumab: mechanism of action, resistance and future perspectives in HER2-overexpressing breast cancer. *Ann Oncol* 2007;18:977–84.
41. Osborne CK, Shou J, Massarweh S, Schiff R. Crosstalk between estrogen receptor and growth factor receptor pathways as a cause for endocrine therapy resistance in breast cancer. *Clin Cancer Res* 2005;11:865–70s.
42. Cardoso F, Piccart MJ, Durbecq V, Di Leo A. Resistance to trastuzumab: a necessary evil or a temporary challenge? *Clin Breast Cancer* 2002;3:247–57; discussion 258–9.